

# Optimization of Potential Pulse Anodized $\text{PbO}_x$ Films for Photoelectrochemical Solar Cells

Dipal B. Patel<sup>1,2,\*</sup>, Khushbu R. Chauhan<sup>2</sup>, Yosuke Ishii<sup>1</sup>, Shinji Kawasaki<sup>1,\*</sup> and Indrajit Mukhopadhyay<sup>2,\*</sup>

<sup>1</sup> Department of Life Science and Applied Chemistry, Nagoya Institute of Technology, Nagoya-466-8555, Japan

<sup>2</sup> Solar Research and Development Center, Pandit Deendayal Petroleum University, Gandhinagar-382007, India

**Abstract-** Augmenting design and fabrication of photoactive materials for their efficient use in energy harvesting devices like photoelectrochemical cells (PECs) are of greater importance from global environmental aspects. A novel DC potential pulse voltammetry was employed for the preparation of photoactive nonstoichiometric nanostructured lead oxide ( $\text{PbO}_x$ ) films. DC pulses of different potential steps, duty cycles and anodization time were applied to lead metal electrode for anodization process in alkaline sodium sulphate solution at 80 °C. Effect of variation in the pulse structure on the structural, optical and photoelectrochemical properties of prepared  $\text{PbO}_x$  photoanodes was analysed by XRD, UV-Vis diffused reflectance spectroscopy and photoelectrochemical measurements. XRD confirms the presence of pure  $\alpha$ - $\text{PbO}$  phases with a trace of  $\beta$ - $\text{PbO}$  in potential pulse anodised photoelectrodes. Optical characterizations revealed that the nonstoichiometric  $\text{PbO}_x$  films are of dual bandgap (1.95 and 2.71 eV) in nature and highly dependent on the structure of an applied potential pulse. Photoresponse measurements under chopped light illumination condition in  $\text{Fe}(\text{CN})_6^{4-/3-}$  (pH 9.2) electrolyte showed a stable photoresponse in a wide potential window of ~1.5 V. Photoelectrochemical cell consist of the  $\text{PbO}_x$  photoanode in aqueous electrolyte inveterate  $J_{sc}$  of 3.01  $\text{mA}/\text{cm}^2$  and  $V_{oc}$  of 768 mV with photon conversion efficiency of 0.87%.

**Keywords-** Photoelectrochemical cell, Nonstoichiometric, Photoanode, Potential Pulse, Duty Cycle

## I. INTRODUCTION

Over the years, the development of energy conversion, energy transfer and energy storage devices have been the topic of interest for many researchers. Enormous developments have been made in this direction starting from photoelectrochemical cells<sup>[1]</sup> to the third generation quantum dot solar cells<sup>[2]</sup>. Researchers have come up with new materials<sup>[3]</sup> and new configurations of the devices<sup>[4-7]</sup> for the efficient conversion of the solar energy. At the same time, core-shell type photo electrodes have attracted many researchers in the field of DSSCs<sup>[8]</sup>. Low cost solution processed techniques<sup>[9]</sup> have gained more attention in the fabrication of bulk as well as nanoscale materials. The

nanocrystal excitonic solar cells of Pb compounds such as  $\text{PbS}$ <sup>[10]</sup>,  $\text{PbSe}$ <sup>[11]</sup> and  $\text{PbSSe}$ <sup>[12]</sup> have gained a great interest due to their large exciton Bohr radii and low cost route of fabrication. Different electrochemical anodization techniques have been tried to make photoactive phases of  $\text{PbO}$  out of lead metal<sup>[13]</sup>. Among all the techniques, potentiodynamic anodization is mostly used and hence understood thoroughly<sup>[14]</sup>. Many groups have explored different approaches for anodization, like pulse coupled potentiodynamic<sup>[13]</sup>, potentiostatic and modified window potentiodynamic. Effect of bath temperature and anodization time is also studied by few groups. The  $\alpha$ - $\text{PbO}$  has got more attraction and studied well because of its major contribution to photoactivity compared to  $\beta$ - $\text{PbO}$ <sup>[15]</sup>. Many groups have concluded that (110) plane of the  $\alpha$ - $\text{PbO}$  leads to a better photoactive film. At the same time, few groups have tried to explore electrochemical pulse technique for the fabrication of highly ordered and self-organized nanotube structures of  $\text{TiO}_2$ <sup>[16]</sup>,  $\text{Al}_2\text{O}_3$ <sup>[17]</sup> and anodic aluminium oxide (AAO)<sup>[18]</sup>. Recently, anodized  $\text{PbO}_x$  films were used to understand the charge transport mechanism of PEC cells<sup>[19]</sup>, redox activity of blank ionic liquids<sup>[20, 21]</sup> by using electrochemical impedance spectroscopy and for designing solid state Schottky junction solar cells<sup>[22, 23]</sup>. In spite of many efforts, the photocurrent more than 3-4  $\text{mA}/\text{cm}^2$  and an open circuit photo voltage of 700 mV is still a challenging task.

In this study, we have made an effort to correlate the influence of DC potential pulse structure with that of the photoelectrochemical performances of PECs comprising of  $\text{PbO}_x$  photoanodes. In doing so, we have investigated structural, optical and photoelectrochemical aspects to draw a correlating conclusions for synthesising an efficient photoactive materials for energy harvesting. Here, we will try to address the protagonist of designing an effective electrochemical route for their application in photoelectrochemical cells.

## II. EXPERIMENTAL

### A. Preparation of lead oxide photoanodes

DC potential pulse voltammetry facilitates alteration of

potential steps, duty cycle and anodization time for synthesizing customizable photoactive material for their applications in photoelectrochemical cells and different photoelectric devices. In this study, a well-known three electrode electrochemical cell arrangement with working, counter and reference electrode was used. The as received chemicals NaOH, Na<sub>2</sub>SO<sub>4</sub>, K<sub>4</sub>Fe(CN)<sub>6</sub> and K<sub>3</sub>Fe(CN)<sub>6</sub>, and deionized water (Milli-Q) were used to carry out all the experiments. A lead foil (99.999% pure, Alfa Aesar) having an effective geometric area 0.25 cm<sup>2</sup> was used as a working electrode (WE). A detailed Pb-metal electrode preparation for anodization is discussed elsewhere [24]. A platinum foil (2 cm<sup>2</sup>) and Hg/HgO (3 M KOH) electrodes were used as a counter (CE) and reference electrode (RE), respectively. A 0.1 M NaOH (in 0.1 M Na<sub>2</sub>SO<sub>4</sub>) solution was used as an active electrolyte for the anodization process at 80 °C. Abolition of any organic and inorganic impurities from the surface was confirmed by electrochemical polishing of lead electrode. All the electrochemical experiments were carried out by using a potentiostat/galvanostat (PGSTAT302N, Autolab) equipped with Nova1.9 software.

### B. Optimization of potential pulse

To study the effect of variation in pulse structure on the resultant photoanodes, a customised DC potential pulse voltammetry was designed and used for anodizing lead metal electrodes. In brief, DC potential pulse comprises of three experimental parameters (variables) i.e., step potential, duty cycle and time. Here, duty cycle (in %) can be defined as  $T_{on}/(T_{on}+T_{off})$ , where  $T_{on}$  and  $T_{off}$  are the time of applied potential  $E_1$  and  $E_2$ , respectively. It is worth mentioning here that it's an iterative process requiring photoanode preparation followed by electrochemical characterizations. In the first instance, different combinations of step potentials ( $E_1$  and  $E_2$ ) in the range of observed anodic peaks (-0.4 to 0.7 V) from the cyclic voltammetry were applied keeping 50% of duty cycle and anodization time of 800 s constant. Next, duty cycle was varied as 33%, 50% and 67% for fixed/optimum step potentials ( $E_1=0.6$  V and  $E_2=0.1$  V) for 800 s. Hence, at the end anodization time (700 and 900 s) was tuned by using optimal values of step potentials and the duty cycle (50%). After anodization, the electrodes were washed thoroughly with deionized water and sintered at 130 °C for 30 min in hot air oven.

### C. Characterizations

As mentioned in the preceding section, material preparation and characterizations were parallel processes for efficient utilization of material, energy and time. PbO<sub>x</sub> photoanodes were characterized by XRD (X'Pert PRO, PANalytical) using CuK $\alpha$  radiation with a characteristic wavelength  $\lambda=1.5406$  Å and UV-Vis diffused reflectance spectroscopy (UV-2600, Shimadzu) for their structural and

optical properties. The photoresponse measurements were performed by using (PGSTAT302N, Autolab). Photoelectrochemical solar cell performance was unveiled by I-V (SS50AAA, Photo Emission Tech., Inc. attached with source measure unit (U2722A, Agilent)) characterization.

## III. RESULTS AND DISCUSSION

The effect of different structures of DC potential pulse on PbO<sub>x</sub> photoanodes were analyzed and compared for their structural, optical and photoelectrochemical performances. It is worth denoting the sample IDs from Table 1 for each potential pulse structure used in the analysis.

Table I POTENTIAL PULSE PARAMETERS

Sample ID	$E_1$ (V)	$E_2$ (V)	Duty Cycle (%)	Anodization time (s)
a	0.6	0.1	50	800
b	0.6	0	50	800
c	0.5	0.1	50	800
d	0.6	0.1	33	800
e	0.6	0.1	67	800
h	0.6	0.1	50	700
i	0.6	0.1	50	900

### A. Structural analysis

The XRD patterns of PbO<sub>x</sub> photoanodes prepared by the implication of different potential pulses (as in Table 1) are shown in Fig. 1. It can be seen from Fig. 1 that all the films consist of pure  $\alpha$ -PbO [25] phases with a trace of  $\beta$ -PbO. One can observe that the intensity of most prominent peak i.e. (110) greatly depends on potential step  $E_2$ . Moreover, the intensity of (110) plane for the sample-(a) is maximum with smallest peak of  $\beta$ -PbO (Fig. 1a). On the other hand the difference of  $\pm 0.1$  V in either  $E_1$  or  $E_2$  changes the phase a lot. For sample-(b), the intensity of  $\beta$ -PbO phase is more and the contribution from  $\alpha$ -PbO phases is relatively low compared to other two samples (a and c) prepared for the same duty cycle and time. The effect of duty cycle on the crystallinity of PbO<sub>x</sub> film can be seen from the Fig. 1a, d and e. It was observed that  $T_{off}$  (duration of  $E_2$ ) has a dominant effect on the relative intensity of  $\alpha$ -PbO and  $\beta$ -PbO phases. It can be seen that by increasing  $T_{off}$ , intensity of (110) plane decreases and  $\beta$ -PbO increases (Fig. 1d). Hence, after second stage of iterative process the potential pulse comprising of  $E_1=0.6$  V,  $E_2=0.1$  V and 50% duty cycle was found to be superior amongst the rest. In the last stage of optimization, anodization time was tuned for the preparation of highly crystalline PbO<sub>x</sub> films. XRD spectra of the samples prepared for 700, 800 and 900 s of anodization time are presented in Fig. 1h, a and i, respectively. Interestingly it was found that the 800 s anodization time result into the films with pure

$\alpha$ -PbO phase with minimal contribution from  $\beta$ -PbO or any other assortment phases (Fig. 1a). It was also observed that mix phases start appearing more prominently with further increase in anodization time above 800 s (Fig. 1i).

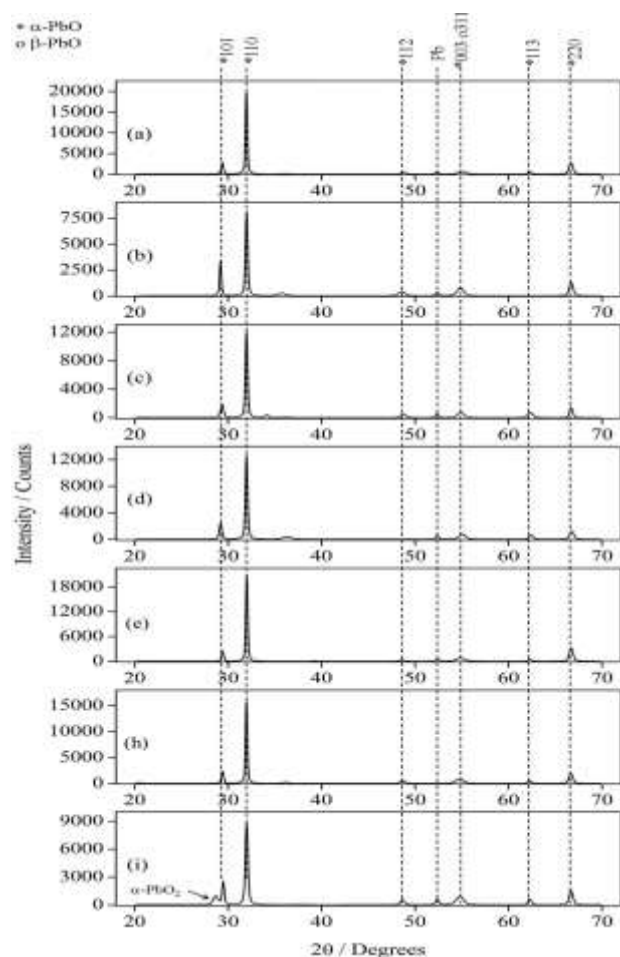


Fig. 1 XRD spectra of anodized lead oxide films through implication of different potential pulse structure

However, the potential pulse technique allowed to synthesis the  $\text{PbO}_x$  films with minimum/no contribution from mixed phases which was difficult to achieve by potentiodynamic anodization method. The structural parameters extracted from the XRD spectrum of  $\text{PbO}_x$  film prepared with optimized potential pulse (i.e. sample-a) are compiled in Table 2. The calculated d-spacing value for (110) plane comes out to be  $2.804 \text{ \AA}$ , which matches very well with the standard  $\alpha$ -PbO phase [25].

Table II STRUCTURAL PARAMETERS EXTRACTED FROM THE XRD SPECTRUM OF SAMPLE-(a)

Parameter (unit)	Value
d-spacing ( $\text{\AA}$ )	2.804
Crystallite size ( $\text{\AA}$ )	500

Micro strain (%)	0.2803
FWHM ( $2\theta$ )	0.1968
Dislocation density ( $\text{cm}^{-2}$ )	$1.27 \times 10^{15}$
Lattice parameter ( $\text{\AA}$ )	$a = 3.97$ & $c = 5.03$

### B. Optical analysis

The optical characterization of the samples can only be carried out by UV-Vis diffused reflectance spectroscopy (DRS) due to opaque lead metal backside. The diffused reflectance spectra of all the samples from 300 to 900 nm are

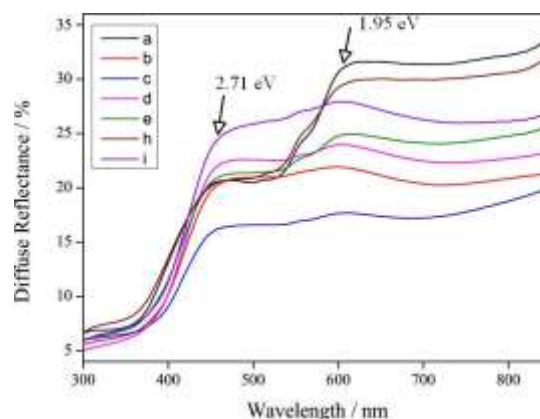


Fig. 2 Diffused reflectance spectra of anodized lead oxide films through implication of different potential pulse structure

shown in Fig. 2. One can notice the existence of dual absorption bands in all the spectra at energies 1.95 and 2.71 eV corresponding to tetragonal ( $\alpha$ ) and orthorhombic ( $\beta$ ) phases of  $\text{PbO}_x$ , respectively. However, the intensities for the absorption at 1.95 eV are not same for all the samples. It is interesting to note that the  $\beta$ -PbO phase absorbs strongly than the  $\alpha$ -PbO. Although XRD pattern does not show any characteristic peak of  $\beta$ -PbO except the peak at  $2\theta = 54.79^\circ$ , which is attributed to both  $\alpha$ -PbO and  $\beta$ -PbO. This anomaly can be explained on the basis of either low crystallinity of  $\beta$ -PbO phase or its minimum content in resulting films. Hence, optical analysis indicates that the anodized films habitually contains photo active  $\alpha$ -PbO phase with impurity of  $\beta$ -PbO. It was further noticed that the contribution of  $\alpha$ -PbO band is comparable with that of  $\beta$ -PbO only in the films prepared by applying potential pulse with  $E_1 = 0.6 \text{ V}$ ,  $E_2 = 0.1 \text{ V}$  and 50% duty cycle for 700 and 800 s (samples-h and a).

### C. Photoelectrochemical analysis

The photoresponse measurements of anodized  $\text{PbO}_x$  films were performed with standard three electrode cell arrangement; anodized  $\text{PbO}_x$  films, Pt foil and  $\text{Hg}/\text{HgO}$  were used as a WE, CE and RE, respectively. PEC cell of the configuration:  $\text{PbO}_x$  film ( $0.25 \text{ cm}^2$ ) |  $0.1 \text{ M K}_4\text{Fe}(\text{CN})_6/0.01 \text{ M K}_3\text{Fe}(\text{CN})_6$  | Pt foil ( $2 \text{ cm}^2$ ) was used to record linear sweep voltammetry under chopped light

illumination condition. It is worth clarifying here that high-density Si photodetector was used for normalizing the energy distribution of the halogen lamp with that of the solar spectrum. All the potentials for PEC studies are denoted with respect to Hg/HgO, 3 M KOH, +0.098 V vs. NHE. The photocurrent variation at different applied potentials under chopped light illumination condition is shown in Fig. 3, 4 and 5. Photoresponse spectra of samples with varying step potentials (b and c), duty cycle (d and e) and anodization time (h and i) are presented (alongside of sample-a for comparison purpose) in Fig. 3, 4 and 5, respectively. Photoelectrochemical window (blocking zone), dark IV characteristic, onset potential ( $V_{on}$ ), photocurrent saturation, maximum photogenerated current ( $I_{ph}$ ) are major key factors to be analysed while investigating photoresponse spectra.

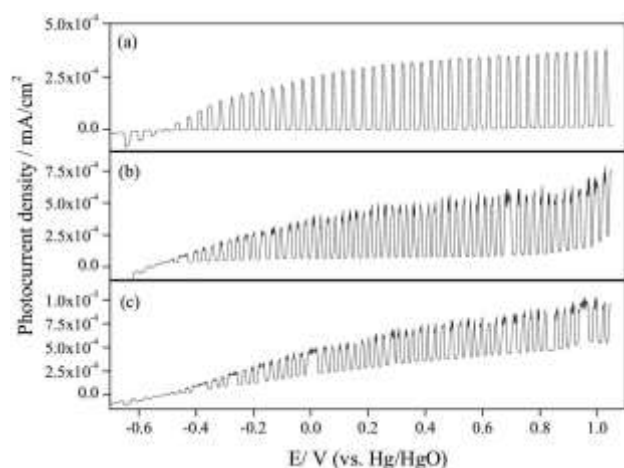


Fig. 3 Photoresponse spectra of samples a, b and c under chopped light illumination conditions. (Fixed parameters: 50% duty cycle and anodization time of 800 s)

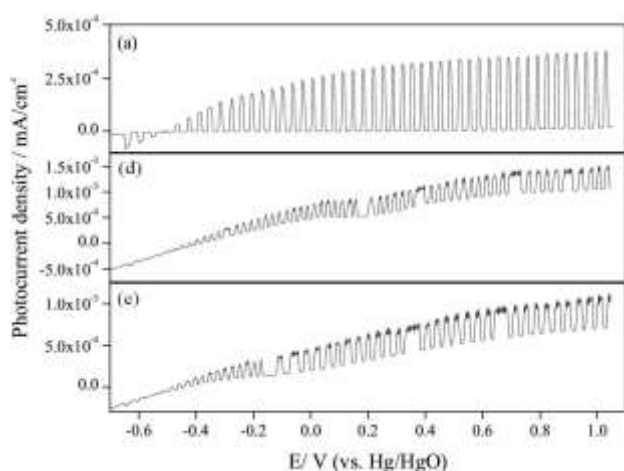


Fig. 4 Photoresponse spectra of samples a, d and e under chopped light illumination conditions. (Fixed parameters:  $E_1=0.6$ ,  $E_2=0.1$  and anodization time of 800 s)

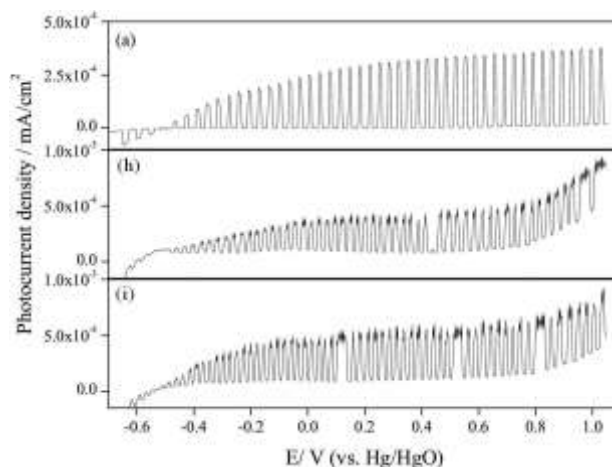


Fig. 5 Photoresponse spectra of samples a, h and i under chopped light illumination conditions. (Fixed parameters:  $E_1=0.6$ ,  $E_2=0.1$  and 50% duty cycle)

Firstly, it can be seen from spectra-a, b, h and i that the nature of the dark IV response reveals the formation of a perfect Schottky barrier at  $PbO_x$ /electrolyte interface. On the other hand spectra of samples-c, d and e showed poor dark IV characteristic. This observation claims the importance of both, step potential  $E_1$  (0.6 V) and a duty cycle (50%). It is worth mentioning here that anodization time (as in Fig. 5) does not have a major impact on the dark IV characteristic. However, time dependent photoanode saturation is clearly visible from Fig. 5a, h and i. The photocurrent spectrum of sample-a achieves the maxima at an applied bias of 1 V with an onset potential ( $V_{on}$ ) for anodic photocurrent is observed at -0.52 V with a blocking zone of ~1.5 V (-0.52 to 1 V).

#### D. Photoelectrochemical Solar cell

PEC cell consisting of optimized  $PbO_x$  photoanode in an active electrolyte of  $Fe(CN)_6^{4-/3-}$  (pH 9.2) was characterized for energy conversion efficiency. The IV curve recorded

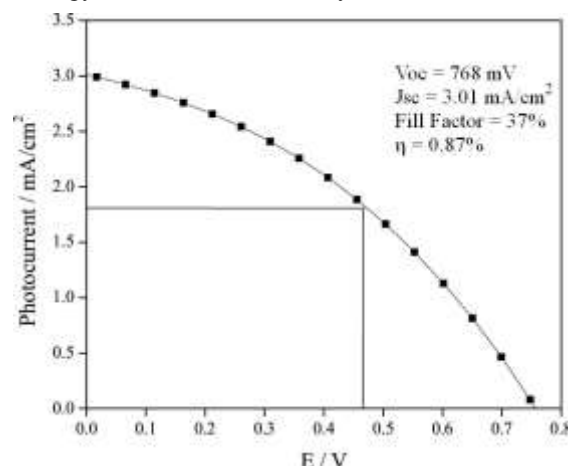


Fig. 6 JV characteristic of the  $PbO_x$  electrode in  $Fe(CN)_6^{4-/3-}$  (pH 9.2) upon illumination of 100 mW/cm<sup>2</sup> light intensity.

under AM-1.5 spectrum is presented in Fig. 6, which shows the ability of the PEC cell made out of anodized  $\text{PbO}_x$  electrode as an energy converting device. IV characteristic was further analyzed to determine the crucial solar cell parameters. The present  $\text{PbO}_x$  based PEC cell is capable of photon to electron conversion efficiency of 0.87% with  $V_{oc}$  of 768 mV and  $3.01 \text{ mA/cm}^2$  current density ( $J_{sc}$ ). Thus, we provided an efficient electrochemical route for synthesizing high performing, nonstoichiometric photoactive material for energy conversion application.

#### IV. CONCLUSION

In the conclusion, we demonstrated a modified electrochemical DC potential pulse technique for synthesizing conventional metal oxides with improved photoactivity. The structure of potential pulse found to have a major impact on the structural, optical and photoelectrochemical properties of the lead oxide films. Stoichiometry and the contribution from the photoactive phases of any metal oxide material can be controlled to improve the PEC cell performance. A highly stable  $\text{PbO}_x$  films having large photoelectrochemical window of 1.5 V was further utilized in PEC solar cell with an energy conversion efficiency of 0.87% with 768 mV of  $V_{oc}$  and  $3.01 \text{ mA/cm}^2$  current density.

#### ACKNOWLEDGEMENT

D. B. Patel acknowledges the financial and technical support from Public Foundation of Chubu Science and Technology Center through Nagoya Institute of Technology (NITech), Nagoya, Japan. D. B. Patel acknowledges the technical discussion with Prof. Shinji Kawasaki and Prof. Yosuke Ishii at NiTech. D. B. Patel and K. R. Chauhan acknowledge their PhD supervisor Prof. Indrajit Mukhopadhyay, Head (Solar Research and Development Center, PDP, India) for continues support and motivation for research.

#### REFERENCES

- [1]. Kalyanasundaram, K., Solar Cells, 15(2), (1985), 93-156.
- [2]. Chuang, C.-H. M., Brown, P. R., Bulovic, V., and Bawendi, M. G., Nat. Mater., 13(8), (2014) 796-801.
- [3]. Liu, M., Johnston, M. B., and Snaith, H. J., Nature, 501(7467), (2013) 395-398.
- [4]. Chauhan, K. R. and Mukhopadhyay, I., J. Appl. Phys., 115(22), (2014) 224506.
- [5]. Chauhan, K. R., Patel, D. B. and Mukhopadhyay, I., New. J. Chem., 39, (2015) 1979-1985.
- [6]. Chauhan, K. R., Patel, D. B. and Mukhopadhyay, I., ECS Trans., 69, (2015) 1-6.
- [7]. Chauhan, K. R., Patel, D. B. and Mukhopadhyay, I., Proc.of SPIE (2015), 9373, 93730N, San Francisco, California, USA
- [8]. Wang, Y., Lu, J., and Wu, F., Nanoscale Res. Lett., 5, (2010) 1682-1685.
- [9]. Afal, A., Coskun, S., and Emrah Unalan, H., Appl. Phys. Lett., 102(4), (2013) 043503.
- [10]. Yoon, W., Boercker, J. E., Lumb, M. P., Placencia, D., Foos, E. E., and Tischler, J. G., Sci. Rep., 3, 2013, pp. 2225.
- [11]. Leschkies, K. S., Beatty, T. J., Kang, M. S., Norris, D. J., and Aydil, E. S., ACS Nano, 3(11), (2009) 3638-3648.
- [12]. Ma, W., Luther, J. M., Zheng, H., Wu, Y., and Alivisatos, A. P., Nano Lett., 9(4), (2009) 1699-1703.
- [13]. Mukhopadhyay, I.; Raghavan, M.; Sharon, M.; Minoura, H.; Veluchamy, P. J Electroanal Chem., 379(1-2), (1994) 531-534.
- [14]. Mukhopadhyay, I.; Ghosh, S.; Sharon, M. Surf Sci., 384(1-3), (1997) 234-239.
- [15]. Schootmiller, J. C. J Appl Phys. 37(9), (1966) 3505-3510.
- [16]. Chanmanee, Wilaiwan, et al. J. Am. Chem. Soc. 130(3), (2008) 965-974.
- [17]. Lee, Woo, Roland Scholz, and Ulrich Gösele. Nano Lett., 8(8), (2008) 2155-2160.
- [18]. Lee, Woo, and Jae-Cheon Kim. Nanotechnology, 21(48), (2010) 485304.
- [19]. Patel, D. B., Chauhan, K. R. and Mukhopadhyay, I., Phys. Chem. Chem. Phys., 16(38), (2014) 20900-20908.
- [20]. Patel, D. B., Chauhan, K. R. and Mukhopadhyay, I., Phys. Chem. Chem. Phys., 16(41), (2014) 22735-22744.
- [21]. Patel, D. B., Chauhan, K. R. and Mukhopadhyay, I., Chem. Phys. Chem., 16(8), (2015) 1750-1756.
- [22]. Patel, D. B. and Mukhopadhyay, I., J. Phys. D: Appl. Phys. 48 (2), (2015) 025102.
- [23]. Patel, D. B., Chauhan, K. R. and Mukhopadhyay, I., Proc.of SPIE (2015), 9364, 93641V, San Francisco, California, USA
- [24]. Patel, D. B. and Mukhopadhyay, I. Int. J. Adv. Res. Sci. Technol, 3(1), (2014) 44-50.
- [25]. Cards, P. D. F., Powder diffraction file cards, (1987), pp5-561, pp4-686, pp37-517, pp. 23-353.